Electronic Supplementary Information

Experimental section

Materials: Pinewood (PW) board was obtained from Shandong Nature Wood Co, Ltd. (Shandong Province, China). Sodium nitrate ($NaNO_3$), ammonium chloride (NH_4Cl), sodium hydroxide (NaOH), ethanol (C_2H_6O), sodium salicylate ($C_7H_5NaO_3$), trisodium citrate dehydrate($C_6H_5Na_3O_7·2H_2O$), p-dimethylaminobenzaldehyde ($C_9H_{11}NO$), sodium nitroferricyanide dehydrate ($C_5FeN_6Na_2O·2H_2O$) and sodium hypochlorite solution (NaClO) were purchased from Aladdin Ltd. (Shanghai, China). Iron chloride hexahydrate ($FeCl_3·6H_2O$) was purchased from Chengdu Kelong Chemical Regent Co. Ltd. Sulfuric acid (H_2SO_4), hydrogrn peroxide (H_2O_2), hydrochloric acid (HCl), hydrazine monohydrate ($N_2H_4·H_2O$), ethylalcohol (C_2H_5OH) and methanol (CH_4O) were bought from Beijing Chemical Corporation. (China). Chemical Ltd. in Chengdu. All chemical reagents used in this work were not purified further.

Synthesis of Fe_3O_4/PC and PC: In brief, PW was cut into small strips (30 × 10 × 3 mm^3), and washed with methanol and ultrapure water. After being dried, the PW was immersed into the 30 mL 0.1 M $FeCl_3·6H_2O$ solution at 60 °C for 24 h. The soaked PW was then dried at 60 °C overnight. Subsequently, the pretreated samples were calcined at 700 °C for 2 h under an Ar atmosphere to get Fe_3O_4-modified PW-derived carbon (Fe_3O_4/PC). The pure PC was obtained under the same preparation conditions without adding $FeCl_3·6H_2O$.

Characterizations: XRD data were acquired by a LabX XRD–6100 X-ray diffractometer with a Cu Kα radiation (40 kV, 30 mA) of wavelength 0.154 nm (SHIMADZU, Japan). SEM measurements were carried out on a Gemini SEM 300 scanning electron microscope (ZEISS, Germany) at an accelerating voltage of 5 kV. XPS measurements were performed on an ESCALABMK II X-ray photoelectron spectrometer using Mg as the exciting source. The absorbance data of the spectrophotometer were measured on UV-Vis spectrophotometer. TEM image was obtained from a Zeiss Libra 200FE transmission electron microscope operated at 200

kV. Gas chromatography (GC-2014C, SHIMADZU) was utilized to quantitatively detect H_2 and N_2.

Electrochemical measurements: All electrochemical measurements were performed in a H-type cell separated by a treated Nafion 117 membrane with a CHI660e electrochemical workstation (Shanghai, Chenhua). Electrolyte solution was Ar-saturated 0.1 M NaOH with 0.1 M $NaNO_3$, using Fe_3O_4/PC (0.05 cm^3) as the working electrode, a graphite rod as the counter electrode, and a Hg/HgO as the reference electrode. All potentials reported in our work were converted to reversible hydrogen electrode (RHE) scale via calibration with the following equation: E (RHE) = E (vs. Hg/HgO) + 0.0591 × pH + 0.098 V and the current density was normalized by the geometric surface area.

Determination of NH_3: The concentration of produced NH_3 was determined by spectrophotometry measurement with the indophenol blue method (the obtained electrolyte was diluted 20 times).[1] In detail, 2 mL of the diluted catholyte was obtained from the cathodic chamber and mixed with 2 mL of a 1 M NaOH solution that contained salicylic acid and sodium citrate. Then, 1 mL of 0.05 M NaClO and 0.2 mL of 1 wt% $C_5FeN_6Na_2O$ were dropped into the collected electrolyte solution. After standing at room temperature for 2 h, the ultraviolet-visible absorption spectrum was measured. The concentration-absorbance curve was calibrated using the standard NH_4Cl solution with NH_3 concentrations of 0, 0.2, 0.5, 1.0, 2.0 and 5.0 ppm in 0.1 M NaOH. The absorbance at 655 nm was measured to quantify the NH_3 concentration using standard NH_4Cl solutions ($y = 0.34993\ x + 0.02177$, $R^2 = 0.9999$).

Determination of NO_2^-: Griess tests can be applied to determine the remaining NO_2^- concentration in the reaction electrolytes.[2] Firstly, the Griess reagents were prepared by dissolving 0.2 g N-(1-naphthyl) ethylenediamine dihydrochloride, 2.0 g sulfonamide, and 5.88 mL H_3PO_4 in 100 mL ultrapure water. Then, diluting the electrolyte to a measurable concentration range. After that, 1.0 mL of the tested electrolyte was added in to a mixture of 1.0 mL of Griess reagent and 2.0 mL ultrapure water to react at room temperature for 10 min under dark conditions, where an azo dye (magenta) can be formed. The absorbance at 540 nm was measured to

quantify the NO_2^- concentration with a standard $NaNO_2$ solution with different NO_2^- concentrations in 0.1 M NaOH (y = 0.21739 x + 0.03390, R^2 = 0.9994).

Determination of N_2H_4: In this work, we used the method of Watt and Chrisp[3] to determine the concentration of produced N_2H_4. The chromogenic reagent was a mixed solution of 5.99 g $C_9H_{11}NO$, 30 mL HCl and 300 mL C_2H_5OH. In detail, 1 mL of electrolyte was added into 1 mL prepared colour reagent and stirred for 15 min in the dark. The concentration-absorbance curve was calibrated using the standard N_2H_4 solution with concentrations of 0, 0.2, 0.6, 1.0 and 2.0 ppm. The absorbance at 455 nm was measured to quantify the N_2H_4 concentration with a standard curve of hydrazine (y = 0.70054 x + 0.10119, R^2 = 0.9998).

Calculations of FE and NH_3 yield:

The amount of NH_3 (m_{NH3}) was calculated by the following equation:

$$m_{NH3} = [NH_3] \times V$$

FE of NH_3 formation was calculated by the following equation:

$$FE = (8 \times F \times [NH_3] \times V) / (M_{NH3} \times Q) \times 100\%$$

The NH_3 yield rate was calculated using the following equation:

$$NH_3 \text{ yield} = ([NH_3] \times V) / (M_{NH3} \times t \times A)$$

Where F is the Faradic constant (96485 C mol^{-1}), $[NH_3]$ is the NH_3 concentration, V is the volume of electrolyte in the anode compartment (60 mL), M_{NH3} is the molar mass of NH_3 molecule, Q is the total quantity of applied electricity, t is the electrolysis time (1 h) and A is the geometric area of the working electrode (0.5 × 0.5 × 0.2 cm^3).

NO_3^- isotopic labelling experiment: The generated NH_3 was verified by an isotope-labelled tracer experiment using a 0.1 M $^{15}NO_3^-$ as a N source. After 1 h of electroreduction at –0.4 V, the electrolyte in the cathodic chamber was adjusted to 2 with a 0.5 M HCl. After that, the neutralized electrolyte (1mL) was mixed with deuterium oxide (D_2O, 0.1 mL). And the mixture was sealed into a nuclear magnetic resonance (NMR) tube (5 mm in diameter, 600 MHz) for further tests.

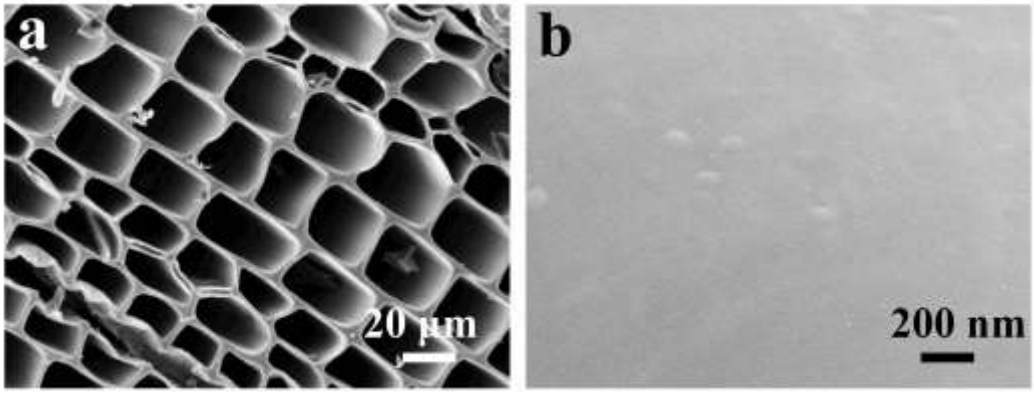

Fig. S1. (a) Low- and (b) high-magnification SEM images of pure PC.

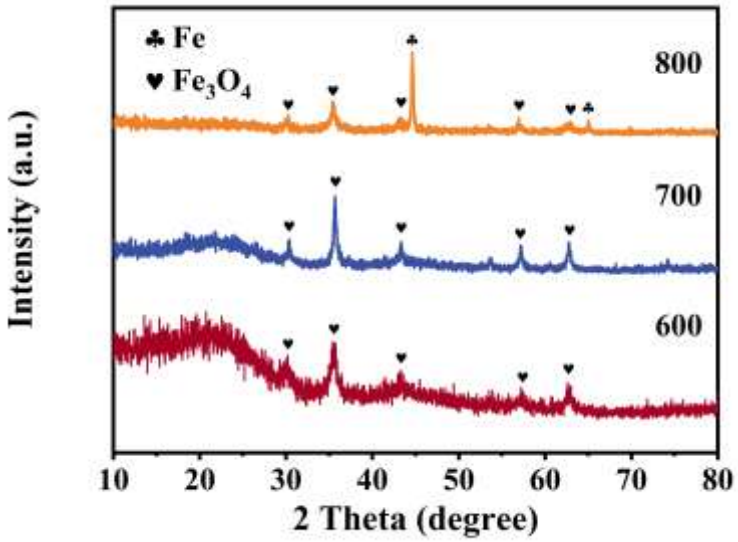

Fig. S2. XRD patterns of Fe_3O_4/PC-600, Fe_3O_4/PC-700, and Fe@Fe_3O_4/PC-800.

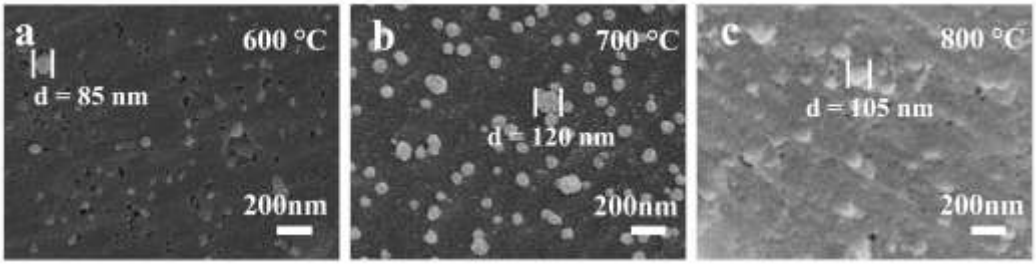

Fig. S3. SEM images of (a) Fe_3O_4/PC-600, (b) Fe_3O_4/PC-700, and (c) Fe@Fe_3O_4/PC-800.

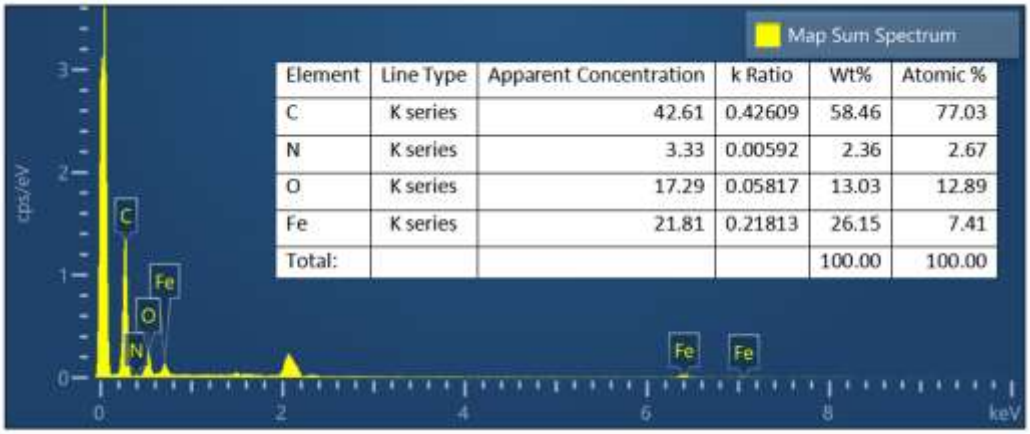

Element	Line Type	Apparent Concentration	k Ratio	Wt%	Atomic %
C	K series	42.61	0.42609	58.46	77.03
N	K series	3.33	0.00592	2.36	2.67
O	K series	17.29	0.05817	13.03	12.89
Fe	K series	21.81	0.21813	26.15	7.41
Total:				100.00	100.00

Fig. S4. EDX spectrum of Fe_3O_4/PC.

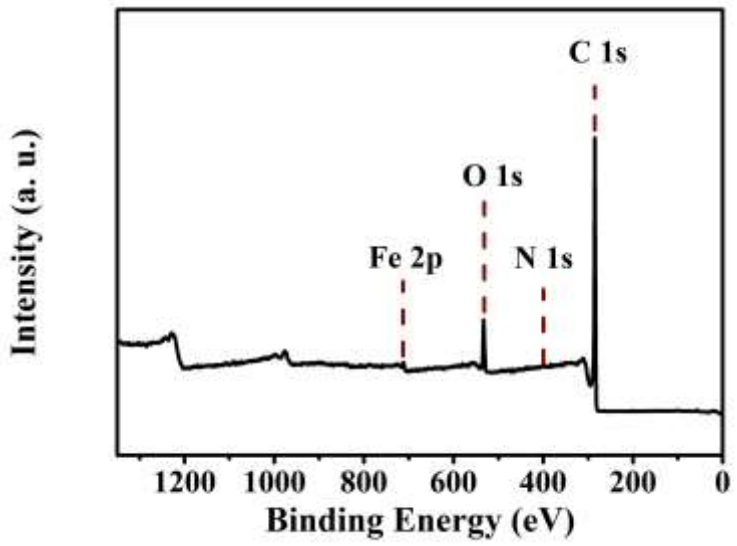

Fig. S5. XPS survey spectrum of Fe_3O_4/PC.

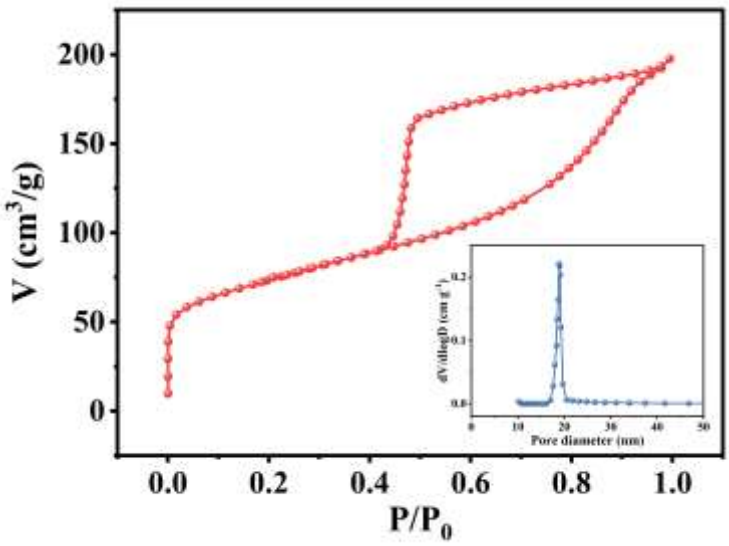

Fig. S6. N_2 adsorption-desorption isotherms and pore-size distribution (inset) of Fe_3O_4/PC.

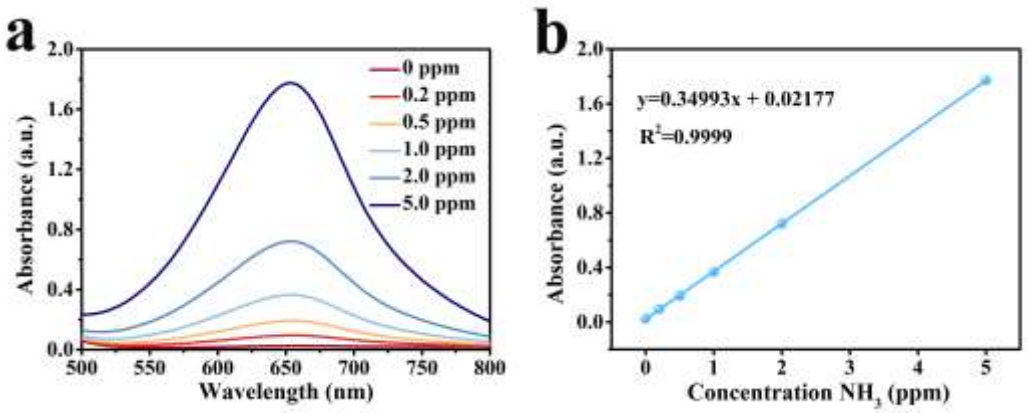

Fig. S7. (a) UV-Vis spectra and (b) corresponding calibration curve for determining NH_3.

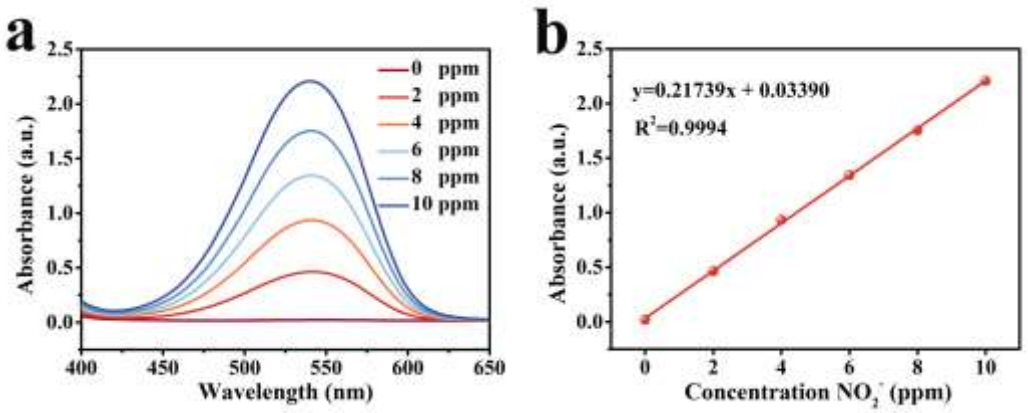

Fig. S8. (a) UV-Vis spectra and (b) corresponding calibration curve for determining NO_2^-.

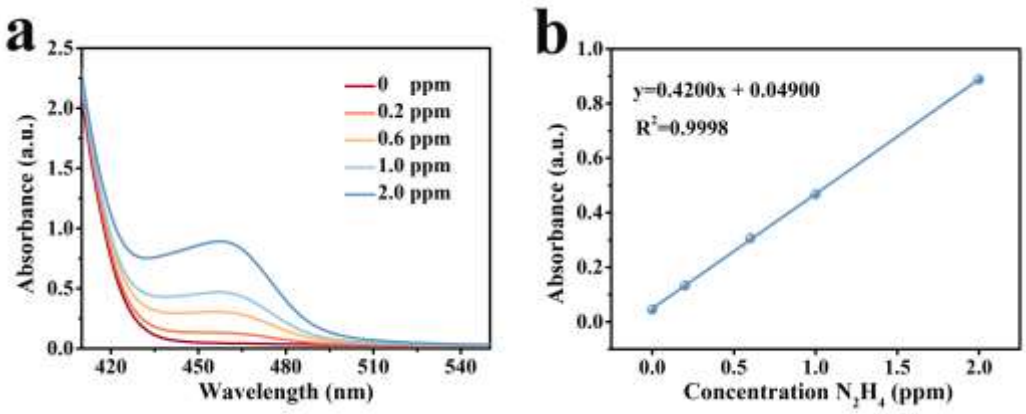

Fig. S9. (a) UV-Vis spectra and (b) corresponding calibration curve for determining N_2H_4.

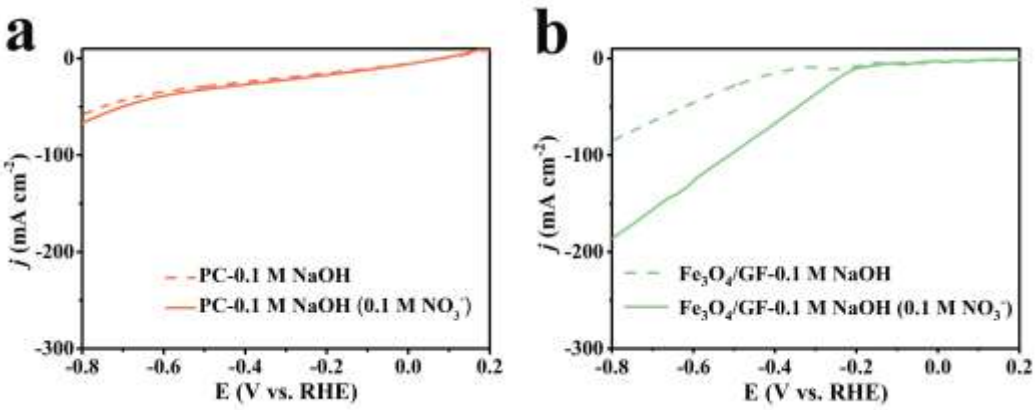

Fig. S10. LSV curves of (a) PC (b) Fe_3O_4/GF for NO_3^-RR in 0.1 M NaOH with/without 0.1 M NO_3^-.

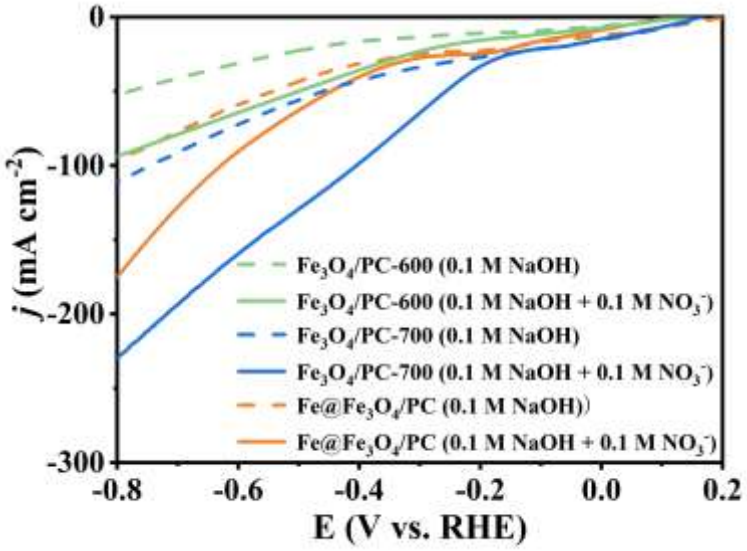

Fig. S11. LSV curves of Fe_3O_4/PC-600, Fe_3O_4/PC-700, and Fe@Fe_3O_4/PC-800 for NO_3^-RR in 0.1 M NaOH with/without 0.1 M NO_3^-.

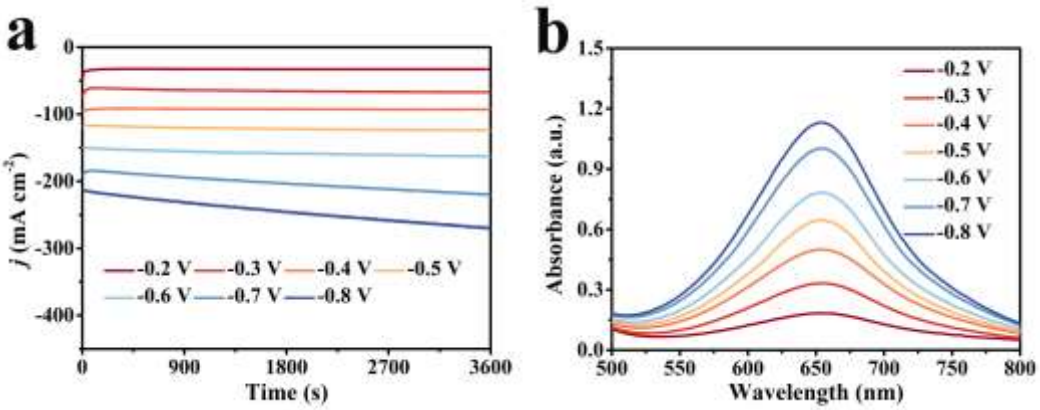

Fig. S12. (a) Chronoamperometry curves of Fe_3O_4/PC at different potentials and (b) UV-Vis spectra of NH_3 produced in the electrolyte at the corresponding potentials.

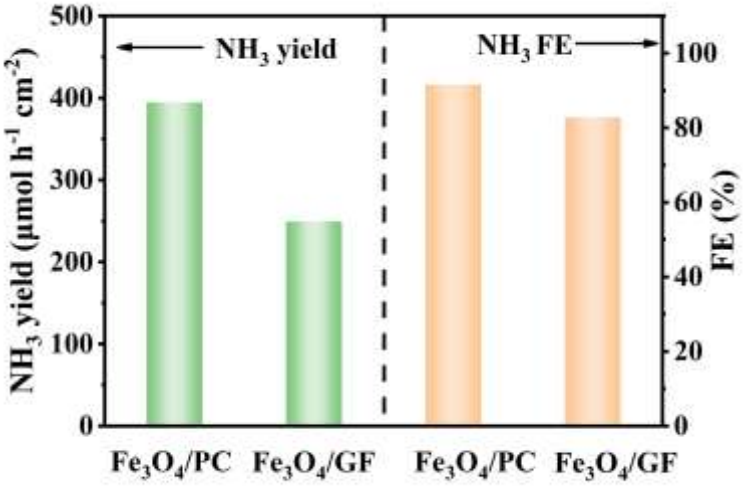

Fig. S13. NH_3 yields and FEs of Fe_3O_4/PC and Fe_3O_4/GF at –0.4 V.

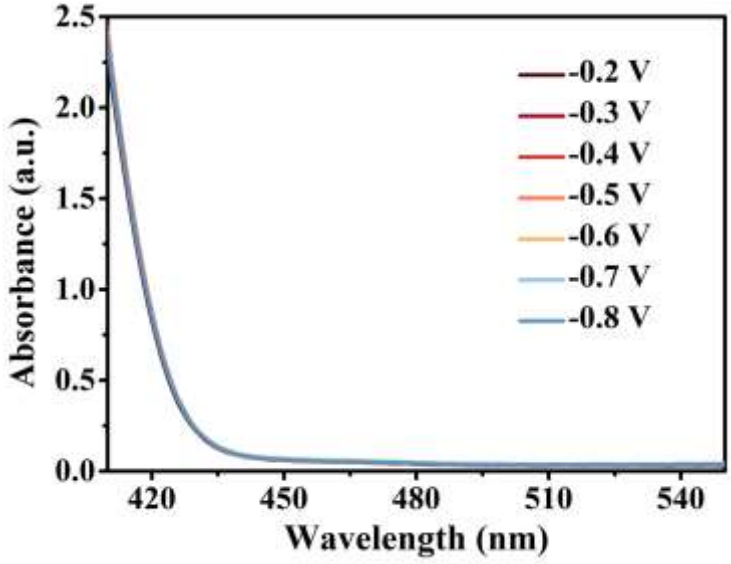

Fig. S14. UV-Vis adsorption spectra of N_2H_4 for Fe_3O_4/PC at each given potential.

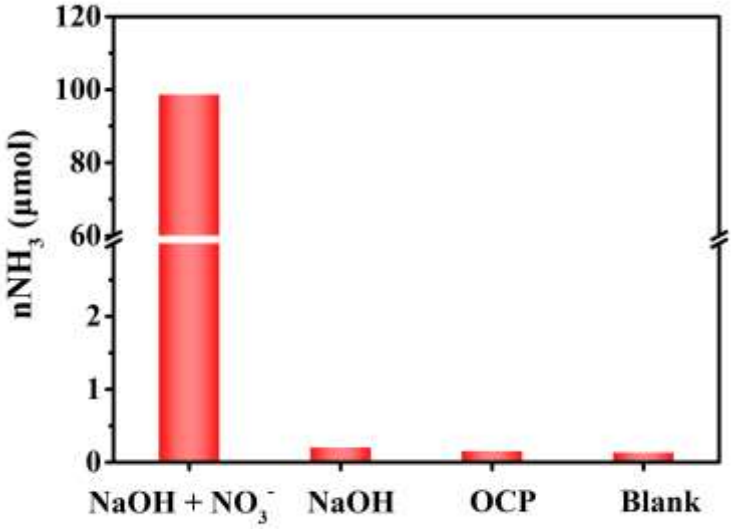

Fig. S15. Comparison of NH_3 yields under different conditions.

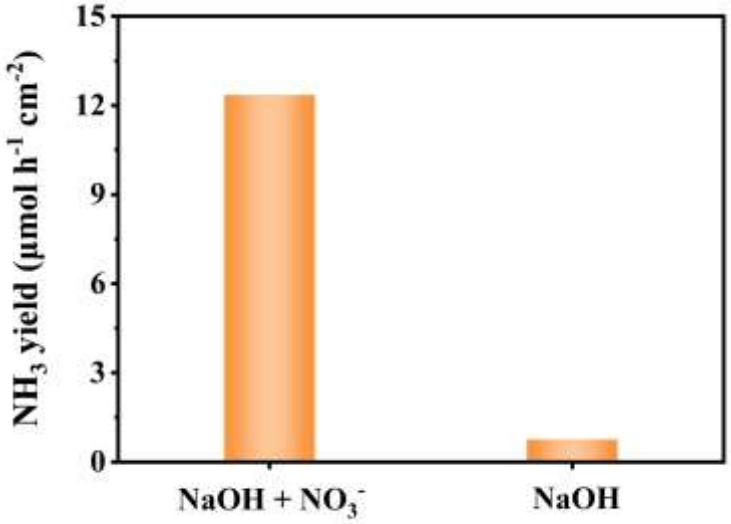

Fig. S16. NH_3 yields of pure PC in 0.1 M NaOH with/without 0.1 M NO_3^- at –0.4 V.

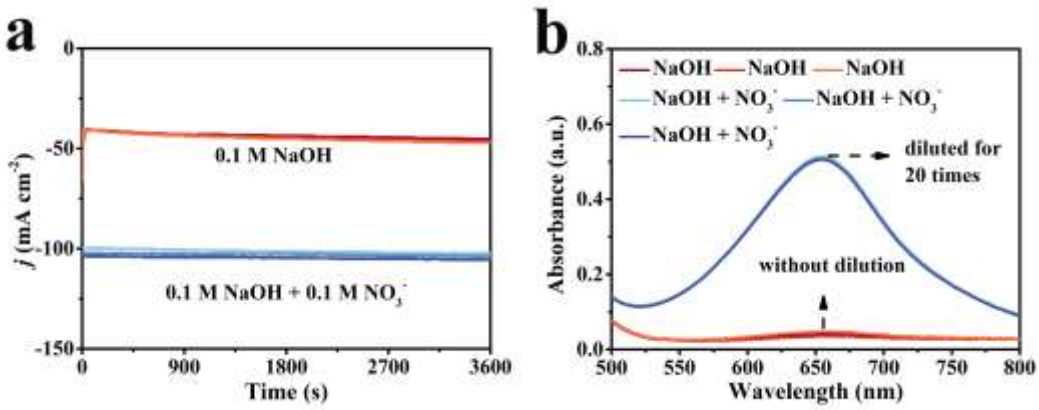

Fig. S17. (a) Chronoamperometry curves and (b) corresponding UV-Vis spectra of NH_3 produced by Fe_3O_4/PC during the alternating cycle tests between NO_3^--containing and NO_3^--free electrolytes.

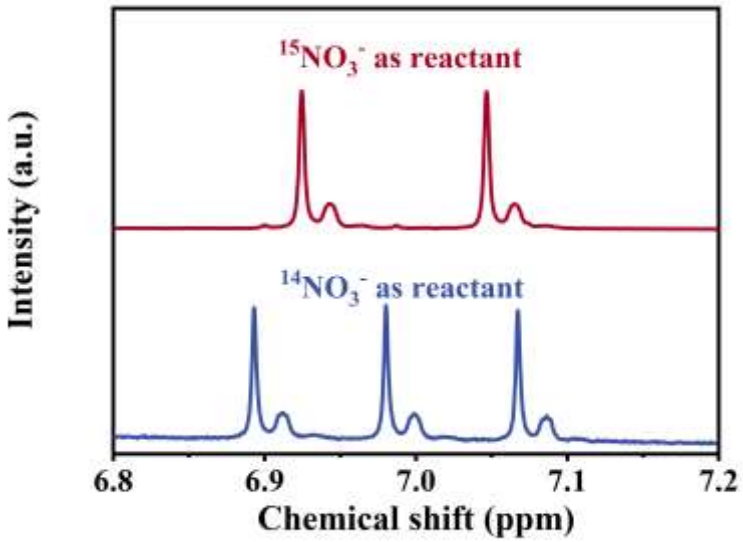

Fig. S18. ^1H NMR spectra for the post-electrolysis electrolyte with $Na^{15}NO_3$ and $Na^{14}NO_3$ as the nitrogen resources.

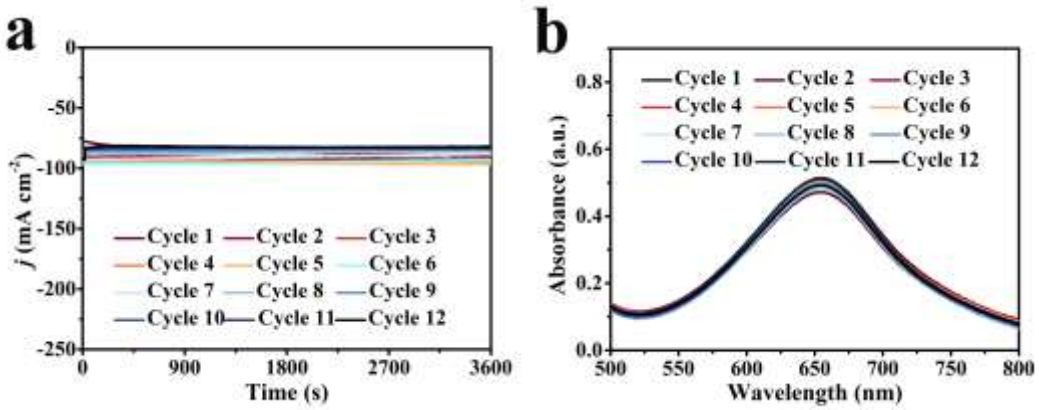

Fig. S19. (a) Chronoamperometry curves and (b) corresponding UV-Vis spectra for generated NH_3 during recycling tests at –0.4 V.

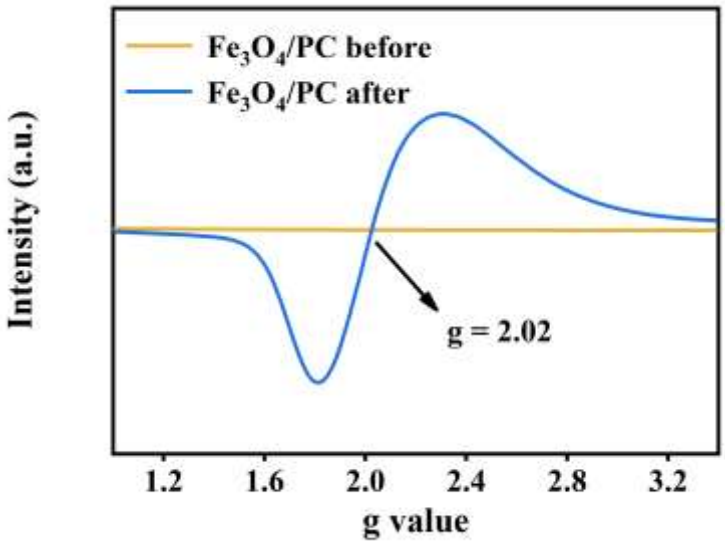

Fig. S20. EPR spectra of Fe_3O_4/PC before and after long-term stability test.

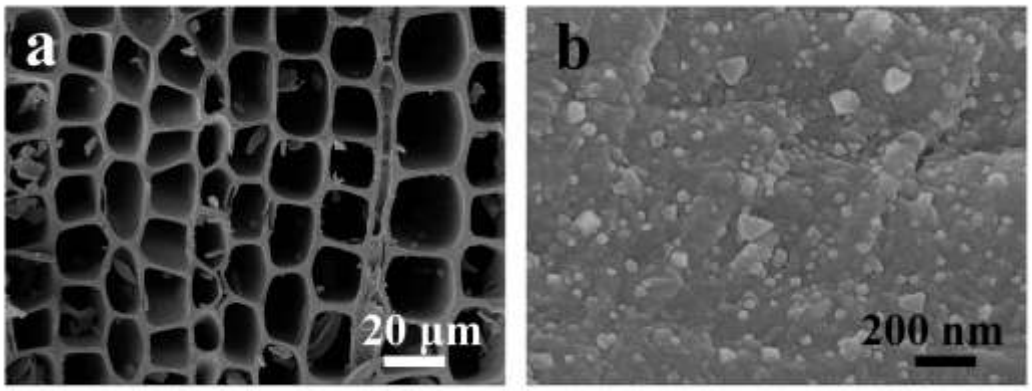

Fig. S21. (a) Low- and (b) high-magnification SEM images of Fe_3O_4/PC after stability test.

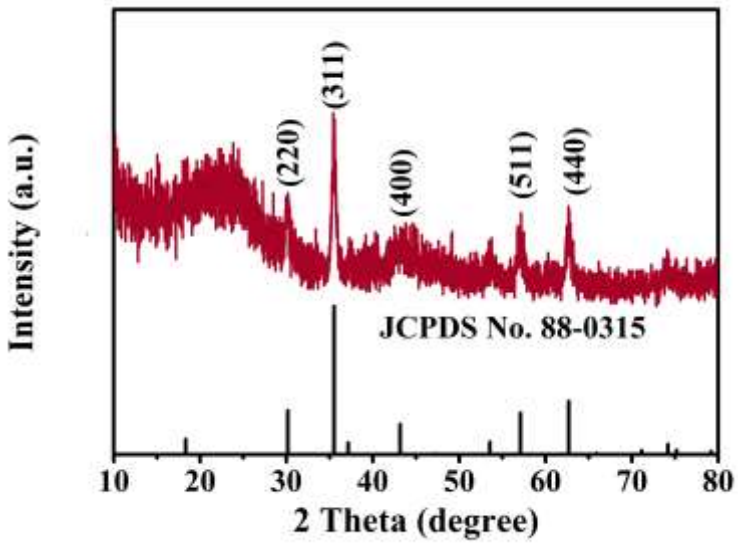

Fig. S22. XRD pattern for Fe_3O_4/PC after long-time electrolysis.

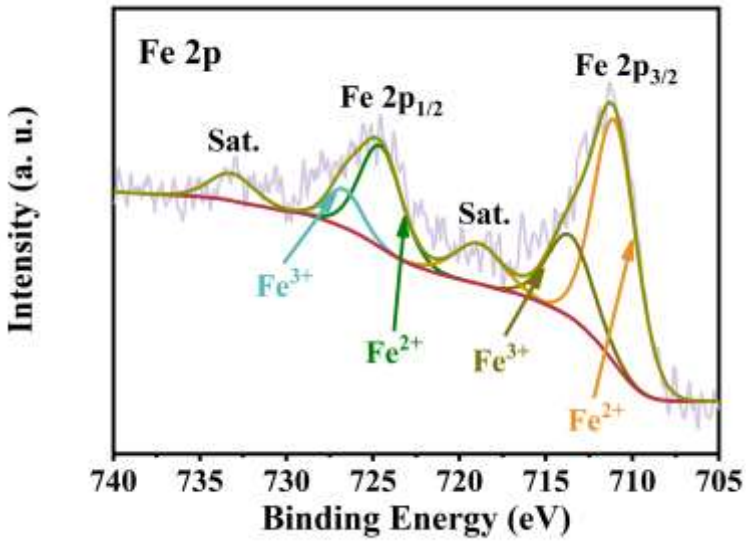

Fig. S23. XPS spectrum of post-electrolysis Fe_3O_4/PC. Based on the integrated peak areas of Fe 2p, the ratio of Fe^{3+}/Fe^{2+} in Fe_3O_4 slightly decreased after the long-term stability test, and a small amount of Fe^{3+} (from 29.63% to 25.62%) transformed to Fe^{2+} (from 70.37% to 74.38%).

Table S1. Comparison of catalytic performance of Fe_3O_4/PC with other reported NO_3^- RR electrocatalysts.

Catalyst	Electrolyte	NH_3 yield	FE (%)	Ref.
Fe_3O_4/PC	0.1 M NaOH (0.1 M NO_3^-)	394.8 μmol h^{-1} cm^{-2}	91.6	This work
Pd facets	0.1 M NaOH (20 mM NO_3^-)	18 μmol h^{-1} cm^{-2}	35.0	4
In-S-G	0.1 M KOH (0.1 M NO_3^-)	1272 μg h^{-1} cm^{-2}	75.0	5
Fe SAC	0.1 M K_2SO_4 (0.5 M NO_3^-)	0.46 mmol $h^{-1}cm^{-2}$	75.0	6
Fe-Co_3O_4/TM	0.1 M PBS (50 mM NO_3^-)	36.7 μmol h^{-1} cm^{-2}	95.5	7
Co-Fe@Fe_2O_3	0.1 M Na_2SO_4 (500 ppm NO_3^-)	1505.9 μg h^{-1} cm^{-2}	85.2	8
Co_3O_4/Co	0.01 M H_2SO_4 (1000 ppm NO_3^-)	260.6 μmol h^{-1} $mg_{cat.}^{-1}$	88.7	9
Co-NCNT	0.1 M NaOH (0.1 M NO_3^-)	352.7 μmol h^{-1} cm^{-2}	92.0	10
CoP/CC	1 M NaOH (0.5 mM NO_3^-)	317 μg h^{-1} cm^{-2}	65.0	11
$Cu_{50}Ni_{50}$	1 M KOH (100 mM NO_3^-)	80.7 μmol $h^{-1}cm^{-2}$	82.0	12
TiO_{2-X}	0.5 M Na_2SO_4 (0.81 mM NO_3^-)	45.0 μmol h^{-1} cm^{-2}	85.0	13
Cu	0.1 M NaOH (20 mM NO_3^-)	/	46.3	14
pCuO-5	0.05 M H_2SO_4 (0.05 M NO_3^-)	292.0 μmol h^{-1} cm^{-2}	89.0	15
BCN@Ni	0.1 M KOH (0.1 M NO_3^-)	140 μmol h^{-1} cm^{-2}	91.2	16

References

1 D. Zhu, L. Zhang, R. E. Ruther and R. J. Hamers, *Nat. Mater.*, 2013, **12**, 836–841.

2 G. W. Watt and J. D. Chrisp, *Anal. Chem.*, 1952, **24**, 2006–2008.

3 L. C. Green, D. A. Wagner, J. Glogowski, P. L. Skipper, J. S. Wishnok and S. R. Tannenbaum, *Anal. Biochem.*, 1982, **126**, 131–138.

4 J. Lim, C.-Y. Liu, J. Park, Y.-H. Liu, T. P. Senftle, S. W. Lee and M. C. Hatzell, *ACS Catal.*, 2021, **11**, 7568–7577.

5 F. Lei, W. Xu, J. Yu, K. Li, J. Xie, P. Hao, G. Cui and B. Tang, *Chem. Eng. J.*, 2021, **426**, 131317.

6 Z.-Y. Wu, M. Karamad, X. Yong, Q. Huang, D. A. Cullen, P. Zhu, C. Xia, Q. Xiao, M. Shakouri, F.-Y. Chen, J. Y. Kim, Y. Xia, K. Heck, Y. Hu, M. S. Wong, Q. Li, I. Gates, S. Siahrostami and H. Wang, *Nat. Commun.*, 2021, **12**, 2870.

7 P. Wei, J. Liang, Q. Liu, L. Xie, X. Tong, Y. Ren, T. Li, Y. Luo, N. Li, B. Tang, A. M. Asiri, M. S. Hamdy, Q. Kong, Z. Wang and X. Sun, *J. Colloid Interface Sci.*, 2022, **615**, 636–642.

8 S. Zhang, M. Li, J. Li, Q. Song and X. Liu, *Proc. Natl. Acad. Sci. U. S. A.*, 2022, **119**, 1–11.

9 F. Zhao, G. Hai, X. Li, Z. Jiang and H. Wang, *Chem. Eng. J.*, 2023, **461**, 141960.

10 J. Chen, Q. Zhou, L. Yue, D. Zhao, L. Zhang, Y. Luo, Q. Liu, N. Li, A. A. Alshehri, M. S. Hamdy, F. Gong and X. Sun, *Chem. Commun.*, 2022, **58**, 3787–3790.

11 H. Zhang, G. Wang, C. Wang, Y. Liu, Y. Yang, C. Wang, W. Jiang, L. Fu and J. Xu, *J. Electroanal. Chem.*, 2022, **910**, 116171.

12 Y. Wang, A. Xu, Z. Wang, L. Huang, J. Li, F. Li, J. Wicks, M. Luo, D.-H. Nam, C.-S. Tan, Y. Ding, J. Wu, Y. Lum, C.-T. Dinh, D. Sinton, G. Zheng and E. H. Sargent, *J. Am. Chem. Soc.*, 2020, **142**, 5702–5708.

13 R. Jia, Y. Wang, C. Wang, Y. Ling, Y. Yu and B. Zhang, *ACS Catalysis*, 2020, **10**, 3533–3540.

14 D. Reyter, G. Chamoulaud, D. Bélanger and L. Roué, *J. Electroanal. Chem.*, 2006, **596**, 13–24.

15 R. Daiyan, T. Tran-Phu, P. Kumar, K. Iputera, Z. Tong, J. Leverett, M. H. A. Khan, A. Asghar Esmailpour, A. Jalili, M. Lim, A. Tricoli, R.-S. Liu, X. Lu, E. Lovell and R. Amal, *Energy Environ. Sci.*, 2021, **14**, 3588–3598.

16 X. Zhao, Z. Zhu, Y. He, H. Zhang, X. Zhou, W. Hu, M. Li, S. Zhang, Y. Dong, X. Hu, A. V. Kuklin, G. V. Baryshnikov, H. Ågren, T. Wågberg and G. Hu, *Chem. Eng. J.*, 2022, **433**, 133190.